Bioorganic & Medicinal Chemistry Letters 23 (2013) 3105–3110

Contents lists available at SciVerse ScienceDirect

Bioorganic & Medicinal Chemistry Letters

journal homepage: www.elsevier.com/locate/bmcl

Discovery of novel Jak2–Stat pathway inhibitors with extended residence time on target

Huiping Guan [a], Michelle L. Lamb [a], Bo Peng [a], Shan Huang [a], Nancy DeGrace [a], Jon Read [b], Syeed Hussain [b], Jiaquan Wu [c], Caroline Rivard [d], Marat Alimzhanov [c], Geraldine Bebernitz [c], Kirsten Bell [c], Minwei Ye [c], Michael Zinda [c], Stephanos Ioannidis [a,*]

[a] Department of Cancer Chemistry, Oncology Innovative Medicines Unit, AstraZeneca R&D Boston, 35 Gatehouse Drive, Waltham, MA 02451, USA
[b] Discovery Enabling Capabilities and Sciences-Cells, Protein & Structural Sciences AstraZeneca, Alderley Park, Cheshire SK10 4TG, UK
[c] Department of Cancer Bioscience, Oncology Innovative Medicines Unit, AstraZeneca R&D Boston, 35 Gatehouse Drive, Waltham, MA 02451, USA
[d] DMPK Department, Oncology Innovative Medicines Unit, AstraZeneca R&D Boston, 35 Gatehouse Drive, Waltham, MA 02451, USA

ARTICLE INFO

Article history:
Received 11 January 2013
Revised 18 February 2013
Accepted 25 February 2013
Available online 7 March 2013

Keywords:
Jak
Myeloproliferative neoplasms
N-(1*H*-Pyrazol-3-yl)pyrimidin-2-amines
V617F mutation
Residence time

ABSTRACT

The discovery of the activating mutation V617F in the JH2 domain of Jak2 and the modulation of oncogenic Stat3 by Jak2 inhibitors have spurred a great interest in the inhibition of the Jak2/Stat pathway in oncology. In this Letter, we communicate the discovery of novel inhibitors of the Jak2/Stat5 axis, the *N*-(1*H*-pyrazol-3-yl)pyrimidin-2-amino derivatives. The rationale, synthesis and biological evaluation of these derivatives are reported. Two lead analogs from this series, **6** and **9**, displayed prolonged residence time on Jak2, at enzymatic level. Although **6** and **9** exhibited moderate selectivity in a selected kinase panel, we chose to test these inhibitors in vivo as a consequence to their long residence time. However, extended inhibition of Jak2 due to the long residence time, in the form of inhibiting phosphorylation of downstream Stat5, was not recapitulated in an in vivo setting.

The Jak (Janus kinase)-Stat (Signal transducers and activators of transcription) pathway has attracted great attention in cancer therapy, after the identification of the mutant Jak2 V617F protein, which displayed a pivotal role in myeloproliferative neoplasms.[1] Likewise, the demonstration of modulation of oncogenic Stat3 by Jak2 inhibitors, such as AZD1480, in solid tumors has expanded the potential utility of such agents.[2,3]

Our laboratories have disclosed several Jak-Stat pathway inhibitors.[4–7] Recently, we described the discovery of a series of N^4-(thiazol-2-yl)pyrimidine-2,4-diamines as ATP-competitive Jak2 inhibitors.[6] These inhibitors displayed good activity against Jak2, both in in vitro and in vivo settings, and sufficient selectivity against Jak3. To further expand our SAR efforts, we envisioned the modification by design of the N^4-(thiazol-2-yl)pyrimidine-2,4-diamine scaffold by moving the thiazol-2-yl amino hinge template from the C_4 to the C_2 of the pyrimidine B-ring (Fig. 1). We anticipated that this change would be well tolerated since the interaction of the thiazoly-3-yl amino group with the kinase hinge residues would be retained.

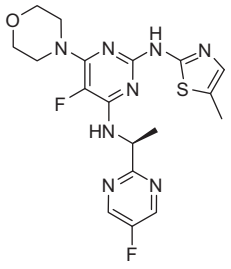

1

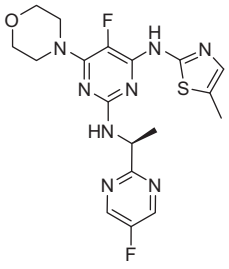

2

Comparing compound **1** versus **2** in the Jak2 enzymatic assay revealed that indeed the change in orientation of the B-ring was tolerated and this analog displayed selectivity against Jak3 at both biochemical and cellular levels as shown in Table 1. We decided to proceed with in vivo screening of compound **1** in nude mice bearing TEL-Jak2 transfected Ba/F3 cells via oral administration (q.d.) at a dose of 10 mg/kg. The percentage (%) downstream inhibition of Stat5 phosphorylation (pStat5) caused by **1** was determined at 2 and 6 h post-dose. In this particular case, some inhibition of pStat5 (~50%) was observed at 2 h while no appreciable inhibition of the phosphorylation was evident after 6 h. Although compound **1** had exhibited significant growth inhibition of TEL-Jak2 cells in vitro (Table 1), its in vivo activity was considered sub-optimal with

* Corresponding author. Tel.: +1 781 839 4556; fax: +1 781 839 4120.
E-mail address: stephanos.ioannidis@astrazeneca.com (S. Ioannidis).

0960-894X/$ - see front matter © 2013 Elsevier Ltd. All rights reserved.
http://dx.doi.org/10.1016/j.bmcl.2013.02.111

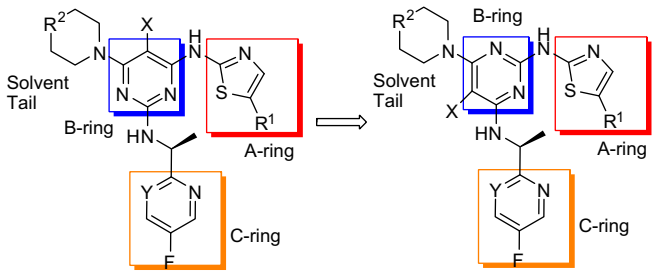

Figure 1. The thiazol-2-yl amino hinge binder.

Table 1
Biochemical and cellular comparison of regioisomeric compounds **1** and **2**, in the Jak2 and Jak3 assays

Compd	Jak2 IC_{50}[a] (μM)	Jak3 IC_{50}[a] (μM)	TEL-Jak2 GI_{50}[b] (μM)	TEL-Jak3 GI_{50}[b] (μM)
1	0.02	16.4	0.03	2.7
2	0.025	>30	0.03	4.9

[a] See Ref. 5 for experimental details. Testing was performed at 5 mM concentration of ATP.
[b] See Ref. 4 for experimental details.

respect to what has been previously observed for **2** in a similar setting.[6] The poor in vivo performance could be attributed to the high metabolic liability of this compound in rodents and high plasma protein binding.[8]

Encouraged by the favorable cellular activity of **1** in the TEL-Jak2 assay, however, we sought to explore the effect of a pyrazol-3-yl amine as a hinge binder motif. We anticipated attenuation of the metabolic liability due to the thiazole ring with the incorporation of pyrazole.[6] The synthesis of analogs with the general structure **3** is depicted in Scheme 1. The synthetic route commenced from 2,4,6-trichloro pyrimidine, which was either commercially available (for R^3 = Cl) or readily accessible (for R^3 = F). First, the solvent tail was attached chemoselectively at the C_4 position of the pyrimidine B-ring at low temperature. Executing the initial step at cooler temperatures as well as ensuring the slow addition of the amine, we secured the mono-addition of the solvent tail onto the pyrimidine B-ring. Addition of the C-ring proceeded at elevated temperature, resulting in mixtures of C_2 and C_6 adducts.

The two regioisomers were readily separated by either liquid chromatography or Super Critical Fluid Chromatography (SFC). The desired regio-isomer could be assigned unambiguously based upon ^{1}H NMR.[9] With the desired regio-isomer in hand, the synthesis was completed by the attachment of the Boc-protected pyrazole via Buchwald–Hartwig amination conditions,[10] under microwave irradiation. It is noteworthy that the protecting group was removed under the employed experimental conditions.[11] We prioritized incorporation of morpholine as the solvent tail group because, in the past, this ring had resulted in favorable cellular activity. On this basis, several 4-morpholino-*N*-(1*H*-pyrazol-3-yl)pyrimidin-2-amine derivatives were prepared and screened in both enzymatic and primary cellular assays (Table 2). As seen in Table 2, the presence of the Me substituent at R^1 seems to secure optimal cellular activity in the TEL-Jak2 assay. Comparison of close analogs **5** (X = N) and **6** (X = O) seemed to indicate discrimination in Jak3 enzymatic activity with preference to compound **5**. A similar behavior was observed for the other matching pair of **7** and **8**, where the oxygen analog **8** exhibited poorer selectivity for Jak3 in the biochemical assay. However, this trend did not seem to translate into the cellular context, and similar selectivities were observed for both X = N and X = O. Obviously there was no significant difference in Jak2 activity in examples **5**–**10**, while the nature of R^3 substituent (e.g., **11** vs **5** and **12** vs **7**) did not seem to affect the enzymatic activities of either Jak2 or Jak3. Interestingly, the cellular potency of analog **11**, in the TEL-Jak2 assay, seemed to be affected due to the lack of a halogen at the R^3 position. At this stage we considered that the cellular activity versus Jak2 was favorable, however we were still concerned with the Jak3 activity being in the nanomolar range.

Comparison of derivative **5** with previously reported[2] *N*^{2}-(1-(5-fluoropyrimidin-2-yl)ethyl)-*N*^{4}-(5-methyl-1*H*-pyrazol-3-yl)-6-morpholinopyrimidine-2,4-diamines **13** and **14** suggests that the lack of substituent α-to the pyrazol-3-yl amine can have a significant effect on Jak3 versus Jak2 selectivity on a biochemical level (Fig. 2).

Further testing revealed that compounds **6** and **9** were competitive inhibitors of Jak2 with K_i's of 0.72 ± 0.005 and 1.41 ± 0.18 nM.

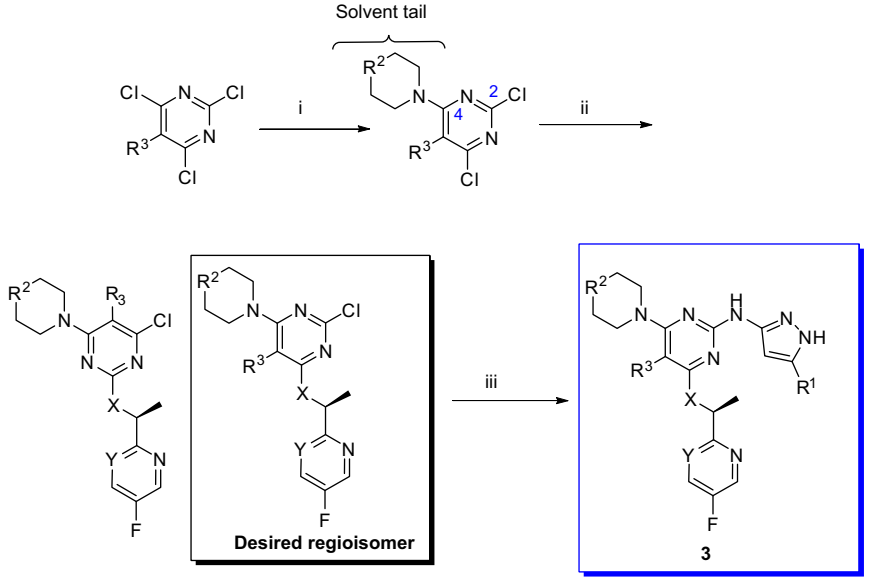

Scheme 1. Preparation of analogs **3**. Reagents and conditions: (i) Amine (such as morpholine), EtOH, −20 °C; (ii) for X = N: amine such as (*S*)-1-(5-fluoropyridin-2-yl)ethanamine, hydrochloride DIPEA, *n*-BuOH, 130 °C, o/n. For X = O: alcohol such as 1-(5-fluoropyridin-2-yl)ethanol *t*-BuOH, *t*-BuOK, 50 °C, o/n. and (iii) Boc-protected pyrazole, $Pd_2(dba)_3$, BINAP, Cs_2CO_3, 180 °C.

Table 2
Biochemical and cellular evaluation of 6-morpholino-N^2-(1*H*-pyrazol-3-yl)pyrimidin-2-amine derivatives **4**–**12**

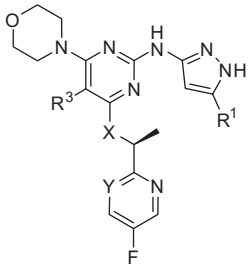

Compd	R^1/R^3	X/Y	Jak2 IC_{50}[a] (μM)	Jak3 IC_{50}[a] (μM)	Tel-Jak2 GI_{50}[b] (μM)	Tel-Jak3 GI_{50}[b] (μM)
4	OMe/F	NH/N	0.037	11.23	0.16	9.4
5	Me/F	NH/N	0.003	0.229	0.015	0.39
6	Me/F	O/N	<0.003	0.020	0.006	0.69
7	Me/F	NH/CH	0.006	0.262	0.019	0.85
8	Me/F	O/CH	0.004	0.087	0.016	0.24
9	Me/F	NH/CF	0.003	0.008	0.009	0.30
10	Me/F	O/CF	0.004	0.045	0.010	0.43
11	Me/H	NH/N	0.005	0.095	0.058	n.d
12	Me/Cl	NH/CH	0.006	0.262	n.d	n.d

[a] See Ref. 5 for experimental details. Testing was performed at 5 mM concentration of ATP.
[b] See Ref. 4 for experimental details.

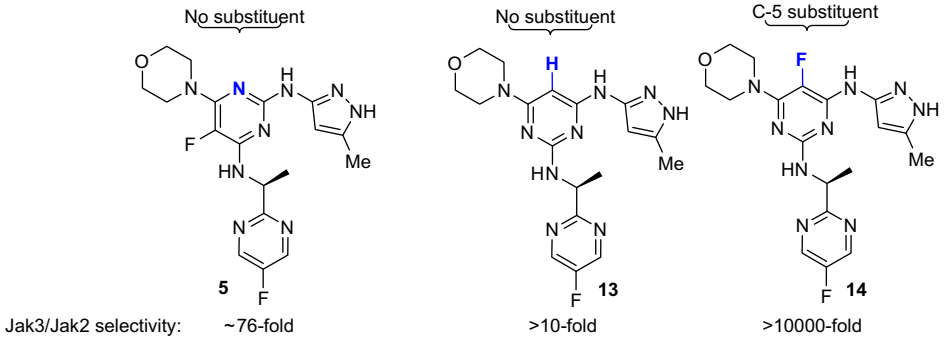

Figure 2. Impact of the presence or absence of a substituent next to the pyrazol-3-yl amino hinge binder on Jak3 versus Jak2 selectivity.

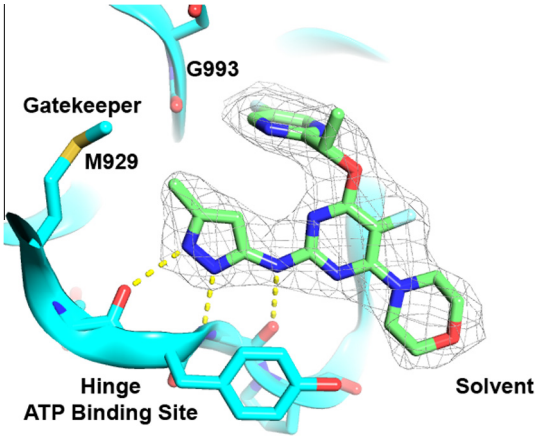

Figure 3. X-ray crystal structure of compound **6** in complex with human JAK2 kinase domain (PDB code: 3zmm). The structure is oriented with the N-terminal lobe towards the top left, the C-terminal lobe towards the bottom right and the hinge region on the bottom left. Selected atoms from the protein are represented as sticks and cartoon in cyan. Compound **6** is shown in green. Hydrogen bonds are shown as dotted yellow lines. Electron density ($2F_o - F_c$), contoured at 1σ, is shown as a wire mesh. Main chain for the P-loop above the plane of the figure has been omitted for the purposes of clarity.

Confirmation of compound **6** being ATP-competitive was obtained after co-crystallization with the ATP-binding domain of Jak2. The X-ray of the interaction of the pyrazol-3-yl amine with the hinge is shown in Figure 3. The heteroaryl C-ring occupies the hydrophobic pocket created by a leucine, stacking the 5-fluoro substituent against the glycine prior to the activation loop. The morpholine ring is positioned towards the solvent channel however there was not any distinguishable interaction with the protein backbone.[12]

Our goal was to evaluate the selectivity of this series outside the Jak family. Compound **9** was selected and assessed for selectivity in a panel of 82 different kinases. This compound displayed greater than 500-fold selectivity against 46 of the kinases tested at a concentration of 0.1 μM. The remaining set of kinases exhibited either strong or moderate inhibition at the same concentration. The overall selectivity was determined by estimating the Gini co-efficient for this molecule (Gini co-efficient = 0.54)[13], which indicated a moderate selectivity in this particular panel (Fig. 4).

Lately, the time of engagement between an inhibitor and its biological target has gained attention in the drug discovery field, as long residence time may enhance the observed in vivo efficacy of a compound. According to this paradigm, the pharmacokinetic properties of an inhibitor have less of an impact on the observed pharmacodynamic effect the longer the complex between inhibitor

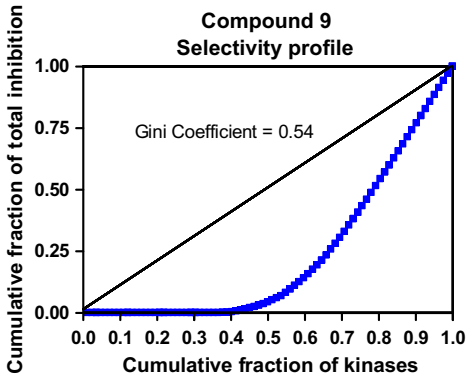

Figure 4. Gini co-efficient of compound **9** in a Millipore panel of 82 kinases, screened at concentration of 0.1 μM. Gini co-efficient can be used as a tool to assess quickly the selectivity of a kinase inhibitor against a large set of kinases and it is independent of ATP concentrations. Particularly, a Gini co-efficient number close to zero would reflect poor selectivity while a number closer to **1** denotes high degree of selectivity versus the set of kinases evaluated.

and target lasts.[14] Thus a fast clearing drug may still achieve appreciable inhibition of the target due to its long residence time. In addition, the combination of long residence time on-target and the simultaneous elimination of the inhibitor from the plasma could allow the amelioration of potential off-target issues. We determined the residence time (t_R) of four compounds with both Jak2 and Jak3 kinase domains, using a rapid dilution enzymatic assay.[15] From Table 6, compounds **6** and **9** displayed much longer residence times for Jak2 than Jak3. In contrast, compounds **5** and **7** exhibited less of a difference between residence times for Jak2 and Jak3. This kinetic observation is opposite to the thermodynamic effect (IC_{50}) that was observed for Jak2 and Jak3. For this reason, compounds **6** and **9** were selected to investigate further in our cascade, despite their moderate selectivity against Jak3 (Fig. 3).

Next, we sought to further explore the SAR in this series by looking into solvent tail replacements for morpholine. Our scope was to identify other solvent tails with improved Jak3 selectivity and possibly longer residence time on Jak2. Table 3 shows examples of the morpholine replacements that were investigated. Compounds **13**–**16** displayed good activity against Jak2 in both enzymatic and cellular settings (data not shown). Examining closely the Jak3 activity, we could discern that morpholine was optimal at the biochemical level for securing selectivity versus Jak3. Particularly in **15** and **16**, a complete loss of selectivity was evident, which, however, seemed to be restored when both of these compounds were evaluated in Tel-Jak2 cellular assay (for both example **15** and example **16** TEL-Jak2 GI_{50} = 0.01 μM). Finally, residence time on Jak2 for these examples was not determined due to the lack of improvement in selectivity versus Jak3, which made them less attractive than the morpholine analogs.

Unable to further improve the selectivity versus Jak3, we evaluated **9** in the Ba/F3 Tel-Jak2 cell line to establish whether the anti-proliferative effect observed in these cells upon treatment would correlate with inhibition of pStat5. Indeed, it was found that the GI_{50} obtained was closely related to the resulting pStat5 IC_{50} value (pStat5 IC_{50} = 0.007 μM). Similarly, the inhibition of Stat5

Table 3
Biochemical and cellular evaluation of (*S*)-5-fluoro-N^4-(1-(5-fluoropyridin-2-yl)ethyl)-N^2-(5-methyl-1*H*-pyrazol-3-yl)pyrimidine-2,4-diamine N^6-substituted derivatives **13**–**16**

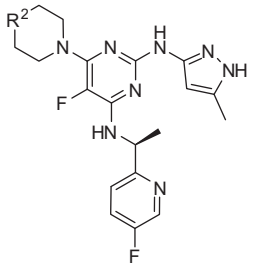

Compd	R^2	Jak2 IC_{50}[a] (μM)	Jak3 IC_{50}[a] (μM)	Tel-Jak3 GI_{50}[b] (μM)
7		0.006	0.262	0.85
13	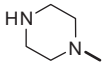	0.004	0.030	0.48
14	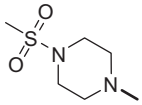	0.003	0.020	0.05
15	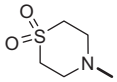	0.003	0.004	0.27
16	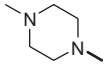	0.017	0.015	0.38

[a] See Ref. 5 for experimental. Testing was performed at 5 mM concentration of ATP.
[b] See Ref. 4 for experimental.

Table 4
V617F data for **6**, **9** and **10**

Compd	TEL-Jak2 GI_{50}[a] (μM)	SET-2 GI_{50}[a] (μM)	UKE1 GI_{50}[a] (μM)
6	0.006	0.078	0.050
9	0.008	0.014	0.022
10	0.010	0.018	0.030

[a] For experimental conditions see Ref. 4.

Table 5
PK parameters for compounds **6** and **9**

Compd	Species	%*F*[d]	AUC (μM × h)	CL (mL/min/kg)	Vdss (L/kg)	Hu Mics (mL/min/mg)	Hu Heps (mL/min/10^6 cells)
6	Rat[a]	74	27.5	11	1.6	<4	<2
	Mouse[b]	64	14.7	17	1.4		
	Dog[c]	56	8.5	13	2.4		
9	Rat[a]	51	17.7	12	3.1	<4	5.2
	Mouse[b]	64	13.3	18	2.9		
	Dog[c]	n.d[e]	n.d	14	2.5		

[a] Han Wistar rat male; 10 mg/kg po (0.1% HPMC); 3 mg/kg iv (DMA/PEG/saline = 40/40/20).
[b] CD-1 mouse female; 10 mg/kg po (0.1% HPMC); 3 mg/kg iv (DMA/PEG/saline = 40/40/20).
[c] Male Beagle; 5 mg/kg po (0.1% HPMC); 2.5 mg/kg iv (HP-β-CD).
[d] Bioavailability was calculated according to the equation $\%F = (AUC_{po} \times Dose_{IV}/AUC_{IV} \times Dose_{po}) \times 100$.
[e] Denotes not tested.

Table 6
Residence time (t_R) for compounds **5**, **6**, **7** and **9** in the ATP-binding site of Jak2 and Jak3 kinases

Compd	Jak2 IC_{50} (μM)	Jak3 IC_{50} (μM)	Jak2 t_R[a] (h)	Jak3 t_R[a] (h)
5	0.003	0.229	2.68	0.98
6	<0.003	0.020	6.65	0.78
7	0.006	0.262	3.20	1.30
9	0.003	0.008	11.07	3.15

[a] See Ref. 15 for experimental procedure.

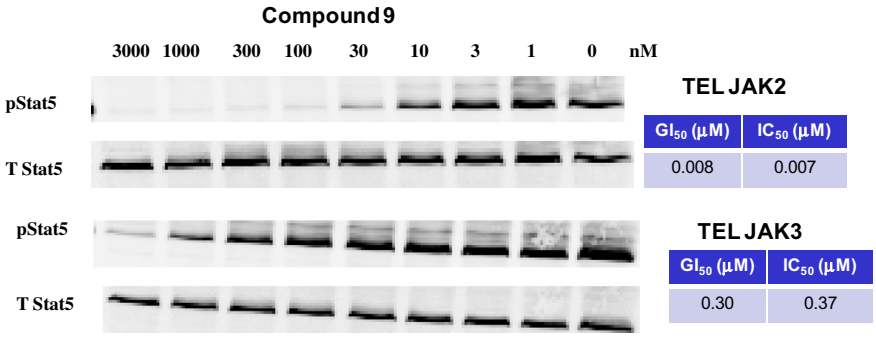

Figure 5. Correlation of anti-proliferative effect with inhibition of Stat5 phosphorylation in TEL-Jak2 and TEL-Jak3 cells, for compound **9**. T = Total, p = phosphorylated.

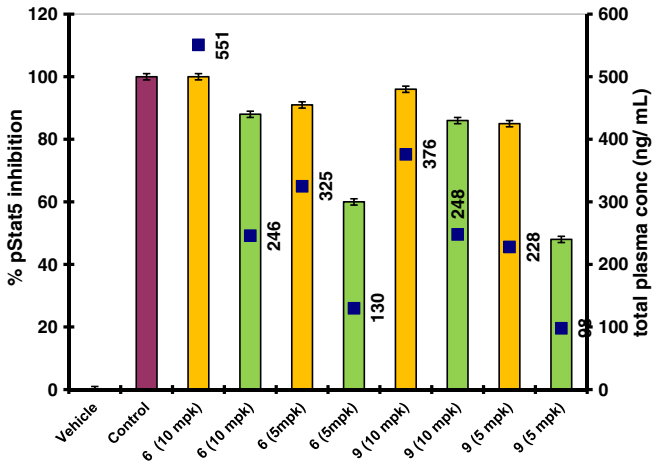

Fig. 6. Pharmacodynamic effect of compounds **6** and **9** on pStat5 in the Ba/F3 TEL-JAK2 mouse model[17] and relationship with plasma pharmacokinetics.[18] The bars represent the average percentage (%) inhibition in phosphorylation of Stat5 (±SD, $n = 3$ for each dose and each time point) and are calculated using vehicle and control inhibitor for maximum and minimum value estimations. The yellow bars correspond to measurement of percentage (%) pStat5 inhibition at 2 h post-dose. The green bars correspond to measurement of percentage (%) pStat5 inhibition at 6 h post dose.

phosphorylation (IC_{50} ~0.37 μM) in the TEL-Jak3 cells indicated a strong correlation with the anti-proliferative effect (Fig. 4). In the more clinically relevant cells, SET-2 and UKE-1, compounds **6**, **9** and **10** inhibited effectively the growth of cells bearing the V617F mutation (Table 4).[16]

To evaluate the pharmacokinetic properties of this series, compound **6** was dosed both orally and intravenously in rodents and dogs and exhibited high bioavailability (%*F*) and oral exposure, as determined by the area under the curve (AUC). The observed clearance (CL) was low in both rat and mouse, while it was rather moderate in dog. Likewise, the volume of distribution in all three species was on the moderate to low side. A similar profile was observed for compound **9**, as depicted in Table 5. In addition, compound **6** appeared to be metabolically stable in both human microsomes and hepatocytes, while compound **9** was marginally less stable in human hepatocytes.

After administration of compounds **6** and **9** in the allograft Ba/F3 TEL-Jak2 murine model we observed significant inhibition of pStat5 (>80%) 6 h post 10 mg/kg dose (Fig. 5, denoted by the green color bars). Inhibition of Stat5 phosphorylation was still evident after 6 h post a single oral 5 mg/kg dose. Looking at the total plasma concentrations (denoted as squares in Fig. 5) of both compounds at the two different doses, we concluded that there was a substantial quantity still present in plasma even after 6 h. In addition, correcting the plasma concentration with the free fraction in mouse for both **6** ($fu = 0.16$) and **9** ($fu = 0.06$) indicated that the available quantities of both **6** and **9** were higher than the observed GI_{50}'s. Monitoring the inhibition of pStat5 at later time points (8 h) for compound **9** revealed significant inhibition at 10 mg/kg (~70% pStat5 inhibition with total plasma concentration of 123 ng/ml) as well as at 5 mg/kg (~50% pStat5 inhibition with total plasma concentration of 55 ng/ml). Given the PK properties of both **6** and **9** in mice, in combination with the long residence time estimated by in vitro experiments, we expected sustained and significant inhibition of phosphorylation of the downstream Stat5. At this point we were reluctant to attribute the observed pharmacodynamic effect to the long residence time particularly when there seemed to be a rough correlation between the observed plasma concentration and observed pStat5 inhibition (Fig. 6). We would have expected that inhibition of Stat5 phosphorylation would not fade with declining plasma concentration, if there were slow-off kinetics observed for these inhibitors when occupying the Jak2 kinase. However, the good pharmacokinetic properties of **6** and **9** may possibly mask the long residence occupancy of the target. Finally, tolerability studies of both **6** and **9** in rodents revealed a narrow therapeutic index, possibly due to the moderate overall kinase panel selectivity. As a consequence of the tolerability data, progression of these inhibitors through our cascade was halted.

In conclusion, we have described a novel series of N^2-(1*H*-pyrazol-3-yl)pyrimidines that display activity against Jak2. Compounds **6** and **9** from this series were extensively investigated and showed activity in cells harboring the V617F mutation as well as displaying downstream inhibition of Stat5 phosphorylation in TEL-Jak2 cells. These compounds demonstrated selectivity against JAK3 at the cellular level in the nanomolar range, and they were found to have slow-off kinetics for Jak2 compared to Jak3. Testing in vivo in a murine Ba/F3 TEL-Jak2 model did not differentiate between the thermodynamic and kinetic activities of these compounds.

Acknowledgments

The authors would like to thank Jeffrey Varnes and Melissa Vasbinder for useful recommendations during the preparation of this manuscript. Likewise, Jing Dai for PK sample analysis and Nancy Su for ATP competition experiments and Isabelle Green and Hannah Pollard for X-ray crystallography.

References and notes

1. Quintas-Cardama, A.; Vertovsek, S. *Expert Opin. Invest. Drugs* **2011**, *20*, 961.
2. Ioannidis, S.; Lamb, M. L.; Wang, T.; Almeida, L.; Block, M. H.; Davies, A. M.; Peng, B.; Su, M.; Zhang, H.-J.; Hoffmann, E.; Rivard, C.; Green, I.; Howard, T.; Pollard, H.; Read, J.; Alimzhanov, M.; Bebernitz, G.; Bell, K.; Ye, M.; Huszar, D.; Zinda, M. *J. Med. Chem.* **2011**, *54*, 262.
3. Hedvat, M.; Huszar, D.; Herrmann, A.; Gozgit, J. M.; Schroeder, A.; Sheehy, A.; Buettner, R.; Proia, D.; Kowolik, C. M.; Xin, H.; Armstrong, B.; Bebernitz, G.; Weng, S.; Wang, L.; Ye, M.; McEachern, K.; Chen, H.; Morosini, D.; Bell, K.;

Alimzhanov, M.; Ioannidis, S.; McCoon, P.; Cao, Z. A.; Yu, H.; Jove, R.; Zinda, M. *Cancer Cell* **2009**, *16*, 487.
4. Gozgit, J. M.; Bebernitz, G.; Patil, P.; Ye, M.; Wu, J.; Su, N.; Wang, T.; Ioannidis, S.; Davies, A. M.; Huszar, D.; Zinda, M. *J. Biol. Chem.* **2008**, *283*, 32334.
5. Ioannidis, S.; Lamb, M. L.; Davies, A. M.; Almeida, L.; Su, M.; Bebernitz, G.; Ye, M.; Bell, K.; Alimzhanov, M.; Zinda, M. *Bioorg. Med. Chem. Lett.* **2009**, *19*, 6524.
6. Ioannidis, S.; Lamb, M. L.; Almeida, L.; Guan, H.; Peng, B.; Bebernitz, G.; Bell, K.; Alimzhanov, M.; Zinda, M. *Bioorg. Med. Chem. Lett.* **2010**, *20*, 1669.
7. Wang, T.; Ioannidis, S.; Almeida, L.; Block, M. H.; Davies, A. M.; Lamb, M. L.; Scott, D. A.; Su, M.; Zhang, H.-J.; Alimzhanov, M.; Bebernitz, G.; Bell, K.; Zinda, M. *Bioorg. Med. Chem. Lett.* **2011**, *21*, 2958.
8. Rat microsomal CL_{int} = 82 μL/min/mg. Compound **1** exhibited reasonable total plasma concentrations in mice 2 and 6 h post-dose (average of 463 and 185 ng/ml, respectively). The percentage (%) free of compound **1** in humans was measured to be around 3%.
9. The two regioisomers could be distinguished by the use of ^{1}H NMR as shown below.

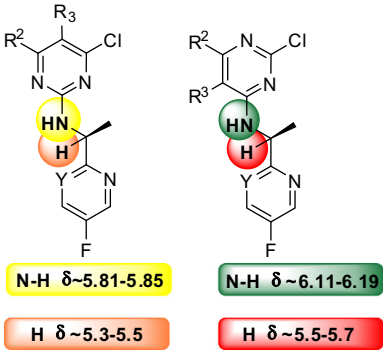

10. For a recent review see: Surry, D. S.; Buchwald, S. L. *Chem. Sci.* **2011**, *21*, 2958.
11. For synthetic experimental see: Guan, Huiping; Hayter, B. R.; Huang, S.; Ioannidis, S.; Johannes, J.; Lamb, M.; Peng, B.; Yang, B. WO 2008132502, 2008.
12. Protein expression and purification, crystallization and cryoprotection procedures have been described previously.[2] Picture of the crystal structure of **6** with Jak2 kinase has been generated by PYMOL.[19] Diffraction data were collected 'in-house' using a Rigaku MM007 X-ray generator equipped with a MAR345 mage plate X-ray detector, using a CuKα radiation at a wavelength of 1.5418 Å focused using Rigaku VariMax HF mirrors. Data were processed using MOSFLM and SCALA and reduced using CCP4 software.[20] The structures were solved by molecular replacement using coordinates of the JAK2 kinase domain (PDB entry 2XA4) as a trial model using CCP4 software. Protein and inhibitor were modeled into the electron density using, COOT[21] and AFITT[22], respectively. The model was refined using Refmac.[23] Atomic coordinates and structure factors for the Human JAK2 complex[24] with compound 6 have been deposited in the Protein Data Bank (3zmm) together with structure factors and detailed experimental conditions.
13. Craczyk, P. P. *J. Med. Chem.* **2007**, *50*, 5773.
14. Lu, H.; Tonge, P. J. *Curr. Opin. Chem. Biol.* **2010**, *14*, 467.
15. Biochemical evaluation of drug–target residence time: The drug–target residence time of JAK2 inhibitors was evaluated using a mobility shift based biochemical assay. Specifically, JAK2 or JAK3 kinase (aa 808–1132, Millipore, catalog # 14–640), peptide substrate (FL-Ahx-IPTSPITTTY FFFKKK-COOH, Primm Biotech, MA, USA), and a particular inhibitor of interest were incubated at room temperature for 30 min. Kinase reactions were initiated by diluting small aliquots of the mixture into solution of ATP in HEPES buffer (75 mM, pH 7.3), and reaction progress was monitored by a Caliper LC3000 system. Initial and steady-state reaction velocities of individual were then derived from each reaction progression curve, and the data were fitted to equation, $p = v_s t + \frac{v_0 - v_s}{k}(1 - e^{-kt})$, where p is the reaction product amount, v_s is the steady-state reaction velocity, t is the reaction time, v_0 is the initial reaction velocity, and k is the rate of transition from v_0 to v_s. The drug–target residence time (t_R) is calculated by the following equation $t_R = \frac{0.693}{k}$.
16. Quentmeier, H.; MacLeod, R. A.; Zaborski, M.; Drexler, H. G. *Leukemia* **2006**, *20*, 471.
17. Nude mice (female) were implanted intravenously with Ba/F3 TEL-JAK2 cells on day 0 and were dosed on day 10. The squares with numbers represent the corresponding average total plasma drug concentration. Mice used in these studies were maintained under specific pathogen-free conditions and were used in compliance with protocols approved by the Institutional Animal Care and Use Committees of AstraZeneca, which conform to institutional and national regulatory standards on experimental animal usage.
18. The pharmacokinetic samples were run on an Applied Biosystems API4000 QTrap using Analyst® software version 1.4.2. The sample analyses were carried out in Sciex#5 LC–MS, using an ACE 3C18 3 μm 20 × 2.1 mm column at ambient temperature and the following eluents: Mobile Phase A: water + 0.1% formic acid + 10 mM ammonium formate B: MeCN + 0.1% formic acid.
19. DeLano, W. L. The PyMOL Molecular Graphics System; DeLano Scientific: San Carlos, CA, USA, 2002. http://www.pymol.org.
20. CCP4 *Acta Crystallogr., Sect. D* **1994**, *50*, 760.
21. Coot; Emsley, P.; Cowtan, K. *Acta Crystallogr., Sect. D* **2004**, *60*, 2126.
22. AFITT: OpenEye Scientific Software, Inc., Santa Fe, NM, USA, http://www.eyesopen.com, 2010.
23. Refmac5: Murshudov, G. N.; Vagin, A. A.; Dodson, E. J. *Acta Crystallogr., Sect. D* **1997**, *53*, 240.
24. Crystallographic statistics for the JAK2 bound to 6 are as follows. Numbers in parenthesis characterize the higher resolution shell. Space group C2, unit cell *a*, *b*, *c* dimensions 44.5, 126.7, 135.6 Å, $\beta = 97.2°$ resolution 17.57 2.50 Å (2.64–20.5 Å), 24425 unique reflections with an overall redundancy of 6.6 (5.9), 95.0% (83.2%) completeness with R_{merge} of 6.5% (30.3%) and mean $I/\sigma(I)$ of 21.0 (5.0). The final model containing 4455 protein, 140 solvent, and 60 compound atoms has an R-factor of 19.3% (R_{free} using 5% of the data 24.6%). Mean temperature factors for the protein and the ligand are 43.0 and 50.1 Å^2, respectively.